ISBN: 978-3-95450-201-1 doi:10.18429/JACoW-IBIC2018-WEPC17

X-RAY PINHOLE CAMERA IN THE DIAGNOSTICS BEAMLINE BL7B AT PLS-II

J. Ko[1†], J. Y. Huang[1], M. Yoon[2], K. Kim[1], B-H. Oh[1], D-T. Kim[1], D. Lee[1], J. Yu[1], and S. Shin[1]
[1]Pohang Accelerator Laboratory, POSTECH, Pohang, Gyungbuk 37673, KOREA
[2]Department of Physics, POSTECH, Pohang, Gyungbuk 37673, KOREA

Abstract

The beam diagnostics beamline BL7B using synchrotron radiation with 8.6 keV critical photon energy from bending magnet has been used to measure the electron-beam size and photon-beam profile on real-time basis. After the completion of the PLS-II, the Compound Refractive Lens (CRL) system was implemented in the optical hutch at BL7B to measure the electron-beam size from X-ray imaging. But we could not have a good image due to short available optical path caused by limited space of the optical hutch. To solve this problem a pinhole camera is implemented in the front-end of BL7B in return for the beamline extension. The progresses on the new x-ray imaging system are introduced in this paper.

INTRODUCTION

After the completion of the PLS-II project [1] to upgrade PLS [2] on March 21, 2012, Pohang Light Source II (PLS-II) is now in full operation. As a result of the upgrade, the PLS beam energy increased from 2.5 GeV to 3.0 GeV, and the stored beam current increased from 200 mA to 400 mA. The emittance is improved from 18.9 nm at 2.5 GeV to 5.8 nm at 3 GeV while the PLS storage ring tunnel structure remains unchanged. In addition, the top-up mode operation is used to stabilize the stored electron beam orbit and the synchrotron radiation flux.

Currently, a total of 31 beamlines including 18 insertion device beamlines are in PLS-II operation for user service. Figure 1 shows the beamline overview of PLS-II. Two multipole wiggler beamlines, three elliptically polarizing undulator beamlines, one planar undulator, twelve in-vacuum undulator beamlines and thirteen bending beamlines have been operated for surface science, magnetic spectroscope, material science, X-ray scattering, XAFS, MX, SAXS, imaging and lithography [3]. In addition to these beamlines, diagnostics beamline BL7B using bending radiation source have been used to measure photon beam stability, electron beam size and real time photon beam profile.

Beamline Overview

The specifications of bending radiation in PLS-II for beam diagnostics beamline BL7B are introduced in Table 1. Bending radiation source is the combined function dipole magnet with 1800 mm length. The central field is 1.46 T and is superposed with the focusing field gradient of -0.4 T/m [4]. The beam size at source point is 60 μm × 30 μm (H × V) and beam divergence at source point is 120 μrad × 2 μrad (H × V). With 3 GeV and 400 mA stored electron beam, photon flux at the critical energy of 8.7 keV is 1.28 ×10^{12} when measured at 15 m from the source point with 1 mm horizontal acceptance.

Unlike typical PLS-II beamline which consists of optical hutch and experimental hutch, beam diagnostics beamline BL7B have only optical hutch and share the optical hutch with the nearby insertion device beamline. Beam diagnostics beamline BL7B do not have the best situation for X-ray imaging due to short optical path length due to limited space, because all optical components are implemented within optical hutch.

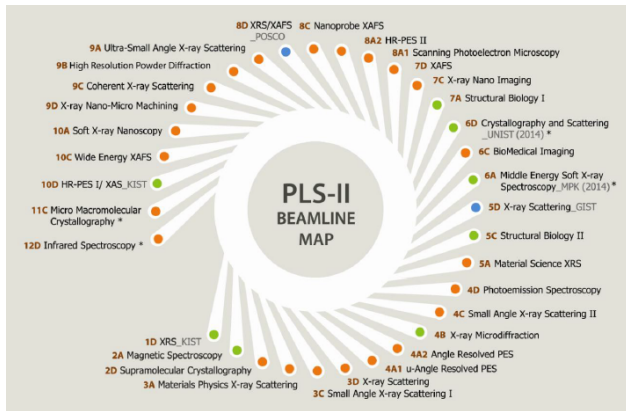

Figure 1: PLS-II beamline map. Here A and C are insertion device beamline, and B and D are bending beamline.

Table 1: The Specifications of Bending Radiation in PLS-II for Beam Diagnostics Beamline BL7B

Parameter	Value	Unit
Electron beam energy	3	GeV
Electron beam emittance	5.8	nm
# of bending magnets	24	
Length of bending magnet	1.8	M
Field / Gradient	1.46/-0.4	(T)/(T/m)
Crit. Photon energy	8.73	keV
Source size (H/V)	60 / 30	μm
Source divergence	120 / 2	μrad

Photon Beam Stability

In order to measure photon beam stability in beam diagnostics beamline BL7B, the most common PBPM [5], that is a simple structure equipped with two blades, is implemented before beam line optics. Figure 2 shows long term slow photon beam motion during 8 days user operation.

† kopearl@postech.ac.kr

ISBN: 978-3-95450-201-1 doi:10.18429/JACoW-IBIC2018-WEPC17

The photon beam motion are described in vertical phase space using two PBPMs in BL7B. By the contribution of slow orbit feedback system and stable thermal loading from top-up operation, long term (8 days) photon beam motion at 13 m from source is within rms 7μm in Fig. 2.

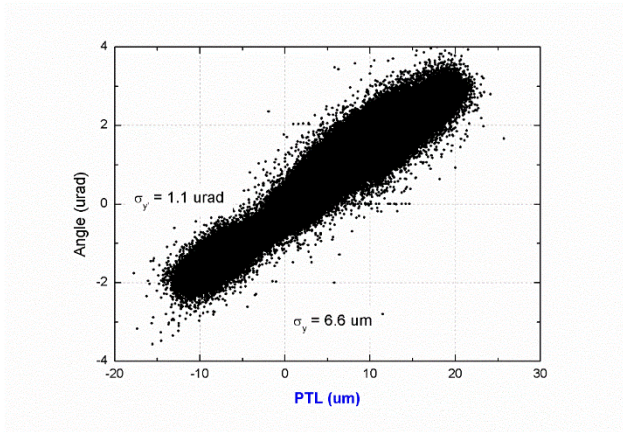

Figure 2: Long term photon beam central motion of PBPM installed at 13 m from the source.

CRL IMAGING SYSTEM

The Compound Refractive Lens (CRL) were implemented in the beam diagnostics beamline to measure the electron-beam size and real time beam profile from X-ray imaging. Figure 3 shows a schematic diagram of the beamline layout. The beamline consist of two PBPMs, channel-cut DCM, CRL, Scintillation crystal and tele-μ-scope. The total length is around 17 m from source to CCD.

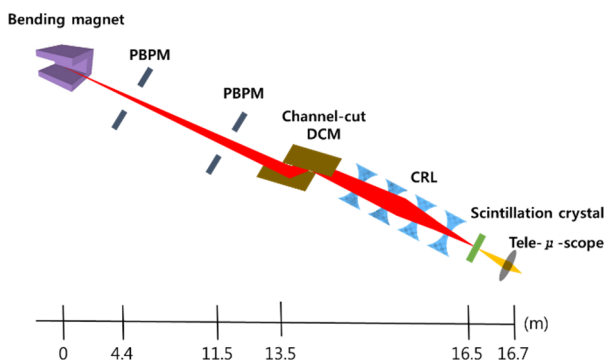

Figure 3: Optical layout of the beamline BL7B.

X-rays are monochromated ($\Delta E / E \approx 10^{-4}$) using a silicon (111) channel cut monochromator located 13.5 m from the source. In order to focus the divergent X-rays, 14 pieces of beryllium parabolic CRLs of diameter 50 μm, positioned just downstream of monochromator, are employed. At that position, the FWHM beam size is 2.1 mm × 0.7 mm. The focal length of each CRL is 2.1 m at 21 keV.

Figure 4 (a) shows image formed on YAG screen for 7 keV X-ray through 200 μm diameter 6 piece CRL system. Normal image has not formed and different images appear on the edge in the figure. This is background effect of high energy X-ray on scintillation crystal after passing through channel-cut DCM and CRL substrate. Therefore, 21 keV 3rd harmonic energy as high energy is considered with 50 μm diameter 14 piece CRL system. As a result, clear image has formed as shown in Fig. 4 (b).

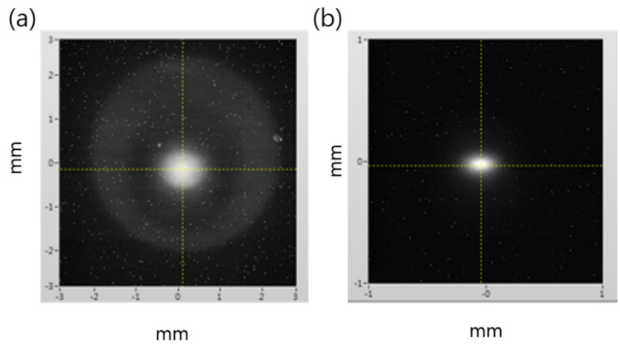

Figure 4: Image on YAG screen. (a) 7 keV and 200 μm CRL. (b) 21 keV and 50 μm CRL.

However, compared with the measured beam size 83 μm and 25 μm (horizontal and vertical) from interferometer that is the conventional method via imaging of the visible synchrotron radiation, the beam size from CRL image is measured as 125 μm and 85 μm for horizontal plane and vertical plane, respectively.

Various causes of beam size measurement error can be deduced as;

- Beam oscillation effect: Measurement error by beam oscillation is inferred with the trend of measured beam size along the shorter exposure time of CCD. Therefore, the measurement with 200 Hz fast acquisition is needed to avoid main oscillation frequencies of storage ring (30 Hz, 60 Hz, 120 Hz, 180 Hz). But the sensitivity is getting worse along shorter acquisition time and at most 10 Hz is highest repetition rate for the measurement. However, measured beam sizes at 10 Hz acquisition are 10 percent smaller than beam sizes measured at 1 Hz for each plane.
- Screen on larger image plane: Mis-position of screen at larger image plane due to limited adjustment range of scintillation crystal.
- Large image demagnification: diffraction error of telescope and measurement error by scintillation crystal thickness enlarge measured beam sizes, since demagnification of x-ray imaging is very large as 0.21 and beam image size on scintillation crystal is at least 5 μm

However, these causes cannot make that big imaging error. One possible reason of large imaging is the deviation of focal length by fabrication error of CRLs. Although we needed to investigate on this more rigorously, the available optical space for finding the final focus was not enough. Therefore, to solve this problem, the CRL system was disassembled and instead a new pinhole camera was installed in the front-end of BL7B.

ISBN: 978-3-95450-201-1 doi:10.18429/JACoW-IBIC2018-WEPC17

PINHOLE IMAGING SYSTEM

A classical pinhole camera set-up has been built at BL7B to measure the electron-beam size and photon-beam profile on real-time basis. From each source point, one ray passes through the pinhole (if it is infinitesimally small) forming an inverted image of the source [6]. A layout of the apparatus is shown in Fig. 5.

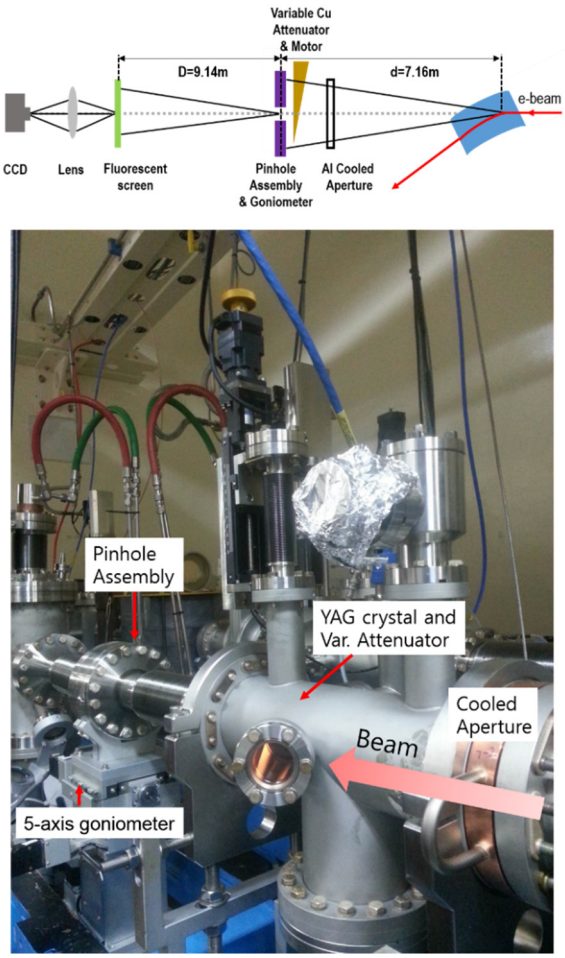

Figure 5: Schematic of the pinhole camera apparatus and system components in front-end.

The X-ray source is the synchrotron radiation coming from the electron beam at the entrance of a bending magnet. The X-rays exit the storage ring vacuum through a 3 mm thick Al window. The pinhole is 1 m downstream of the window and 7.16 m downstream of the source point. After passing through the pinhole, the X-rays strike a fluorescent screen located 9.14m downstream of the pinhole (magnification 1:1.3). Finally, the visible light is imaged with a CCD camera.

The pinhole is quite simple and easy to fabricate. There are actually 5 x 5 rectangular pinholes of various sizes. They are formed using a grid of flat and parallel carbide tungsten plates separated by tungsten wires (Fig. 6). The pinhole assembly is remotely moveable with five degrees of freedom: horizontal (x) translation, vertical (z) translation, rotation around the x, y, and z axes. For the pinhole, one can choose among five horizontal (50, 40, 35, 25, 20 µm) and five vertical (40, 35, 25, 20, 16 µm) sizes. The 500 x 500 µm pinhole is used for alignment purposes. Note that the nonzero penetration of hard X-rays (critical photon energy of 8.73 keV) in tungsten requires the use of a thick pinhole. We are using a 5 mm thick carbide tungsten to block the penetration of high energy x-rays sufficiently. Because of the thickness of the pinhole one should view it like a tunnel rather than a simple hole. With the smallest size aperture, the tunnel presents an aspect ratio of 300 which requires a precise angular adjustment to place it parallel to the incoming X-ray beam. Note that a non-parallelism of the beam with the tunnel axis results in an effective reduction of the aperture.

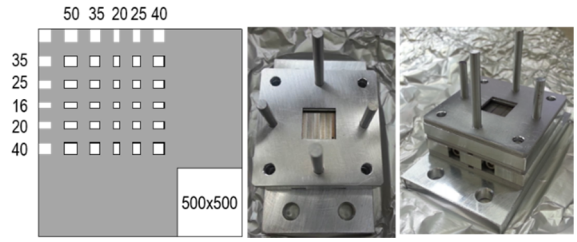

Figure 6: An array of 5 x 5 rectangular pinholes is made with tungsten plates and tungsten wires. The wide pinhole is used for alignment purposes and the small pinholes are used during the measurement.

To acquire and measure the size of the source we image the screen with a tele-µ-scope and CCD. Figure 7 shows an image formed on fluorescent screen (CdWO4) through a 40 x 20 µm pinhole and a two-dimensional Gaussian fitting profiles.

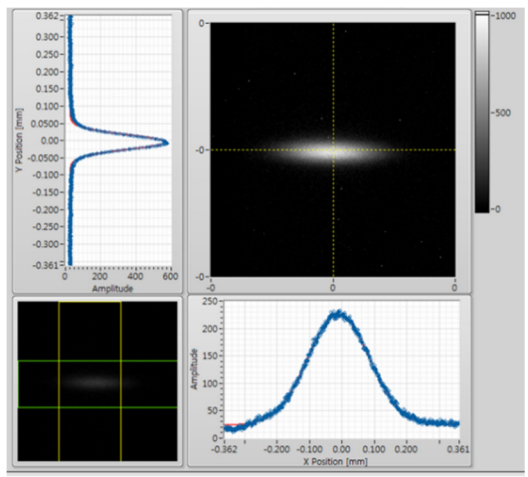

Figure 7: Image on fluorescent screen (CdWO4) through a 40 x 20 µm pinhole and a two-dimensional Gaussian fitting profiles.

Compared with the measured beam size 83 µm and 25 µm (horizontal and vertical) from interferometer, the beam

ISBN: 978-3-95450-201-1 doi:10.18429/JACoW-IBIC2018-WEPC17

size from pinhole camera image is measured as 95 μm and 21 μm for horizontal plane and vertical plane, respectively.

The performance of the measurement of the transverse electron beam size is given by the width of the point spread function (PSF) of the X-ray pinhole camera [7]. The image formed on the camera is the convolution of several independent contributions including beam size, pinhole size, fluorescent screen and CCD. Let us call Σ the r.m.s. Gaussian size of the acquired image and assume the source and the PSF's to be Gaussian. Then Σ can be expressed as follow:

$$\Sigma = \left[\left(S \cdot C_{mag}\right)^2 + S_{aper}^2 + S_{diff}^2 + S_{scr}^2 + S_{CCD}^2\right]^{1/2} = \left[\left(S\frac{D}{d}\right)^2 + S_{sys}^2\right]^{1/2}, \quad (1)$$

where S is the r.m.s. size of the image of the photon emitted by electron beam at the source point, S_{aper} is the geometrical contribution introduced by the finite size of the pinhole, S_{diff} is the diffraction contribution by the small pinhole, S_{scr} is the screen spatial resolution, S_{CCD} is the spread induced by the camera, which includes pixel size, lens aberration and depth of focus through the finite thickness of the screen and aperture of the lens and S_{sys} is effective PSF of the whole pinhole system. C_{mag} is the magnification factor of the pinhole camera. d is the distance from source point to pinhole. D is the distance from pinhole to screen.

To determine the width of system PSF for the pinhole camera a beam based calibration method has been developed in the SSRF storage ring [7]. By varying the beam size S at the source point and measuring image size Σ, the practical S_{sys} can be derived from equation (1) using least-square fitting method. The beam size of source point was changed by modifying the power supply current I_{Q5} of the 5th set of quadrupoles. And the beam size could be described as follow:

$$S_i^2 = \beta_i \epsilon_i + (\eta_i \sigma_\epsilon)^2 , \quad (2)$$

where S_i is the beam size in the horizontal or vertical plane respectively$(i = x,\ y)$, and β_i and η_i are the betatron and dispersion functions at the source point and in the corresponding plane; and ϵ_i and σ_ϵ are the emittance and the relative energy spread of the electron beam.

Figure 8 shows the beam-size according to the pinhole-size. We need to find some correlation between pinhole-size and beam-size in order to verify the usability and reliability of pinhole camera. And then a machine study will also follow to determine the PSF for the pinhole camera described above.

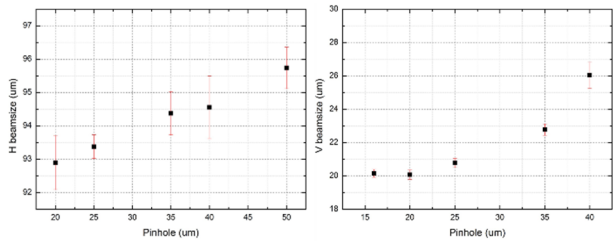

Figure 8: The beam-size according to the pinhole-size for horizontal plane and vertical plane, respectively.

CONCLUSION

The beam diagnostics beamline BL7B takes the important role to provide the information on photon beam condition in PLS-II. Especially, an X-ray pinhole camera has been installed in BL7B and the electron-beam size and photon-beam profile on real-time basis are measured. To optimize the pinhole imaging system, further investigation based on beam based calibration is necessary.

ACKNOWLEDGEMENTS

This research was supported by the Converging Research Center Program through the Ministry of Science, ICT and Future Planning, Korea (NRF-2014M3C1A8048817) and the Basic Science Research Program through the National Research Foundation of Korea (NRF-2015R1D1A1A01060049).

REFERENCES

[1] S. Shin et al., J. Instrum. 8, P01019 (2013).

[2] S. H. Shin, M. Yoon and E.-S. Kim, J. Korean Phys. Soc. 49, 1591 (2006).

[3] See "http://pal.posech.ac.kr/paleng/Menu.pal?method=menuView&pageode=paleng&top=2&sub=3&sub2=1&sub3=0" for the information of PLS-II beamline.

[4] S. Shin et al., J. Instrum. 8, P08008 (2013).

[5] Changbum Kim et al., J. Korean Phys. Soc. 66, 167 (2015).

[6] P. Elleaume, C. Fortgang, C. Penel, *et al,* Measuring beam sizes and ultra-small electron emittances using an X-ray pinhole camera, J. Synchrotron Rad. 2 (1995), 209–214

[7] Y.B. Leng, G.Q. Huang, M.Z. Zhang et al., The beam-based calibration of an X-ray pinhole camera at SSRF. Chin. Phys. C 36, 80–83 (2012)